PREDICTION OF FLOW-INDUCED VIBRATION BEHAVIOUR OF A CIRCULAR CYLINDER IN A UNIFORM STREAM

M.H. Bahmani M.H. Akbari
Department of Mechanical Engineering, Shiraz University, Shiraz, 71348-51154, Iran
hossein459@yahoo.com *akbari@eng.shirazu.ac.ir*

ABSTRACT

In this study the basic characteristics of dynamic response and vortex shedding from an elastically mounted circular cylinder in laminar flow is numerically investigated. The Reynolds number ranges from 80 to 160, a regime that is fully laminar. A vortex method is utilized to solve the 2-D Navier-Stokes equations in terms of vorticity. The effects of mass ratio and damping ratio on the system response are investigated. The numerical results exhibit acceptable agreement with available experimental data.

1. INTRODUCTION

Flow-structure interaction occurs in many engineering fields. A fundamental flow-structure interaction problem is the flow-induced vibration of a structure due to vortex shedding. The case of vortex induced vibration (VIV) of a circular cylinder has been given more attention because of its practical importance (such as in exchangers, marine cables and flexible risers in petroleum production). An elastically–mounted circular cylinder exhibits a range of responses depending on a number of parameters including the reduced velocity, U^*, ($U^*=U f_n /D$, where U, D and f_n are flow velocity, cylinder diameter, and natural frequency of system, respectively), Reynolds number, Re, mass ratio m^* (ratio of cylinder mass to displaced fluid mass, $m^*=(4m)/(\pi\rho D^2 L)$), and damping ratio, ζ, (ratio of damping coefficient to critical damping coefficient, $\zeta = c/c_{critical}$). During vortex-induced vibration lock-in phenomenon may occur, in which the vortex shedding and oscillation frequencies synchronize. This synchronization can lead to an amplification of cylinder's vibrational response.

The practical significance of VIV has led to a large number of studies. Much experimental study has been done on VIV of a circular cylinder. Feng (1968) conducted VIV experiments in an air tunnel. He showed that depending on system parameters (m^*, ζ, U^*, f_n), a range of responses may occur. He also explored the effects of damping on both the amplitude and frequency response. Gharib (1999) has noted the absence of lock-in behavior from almost all experimental studies for small mass ratios.

Khalak and Williamson (1999) carried out VIV experiments using a setup with low mass-damping ($m^*\zeta$). They found that the system response, depending on the magnitude of mass-damping parameter, may be of two different types. Jauvtis and Williamson (2003) studied the behavior of an elastically-mounted cylinder with both streamwise and transverse motions. The range of values of m^* in their study was between 5 and 25. It was found that the freedom of body to oscillate in both directions has very little effect on the transverse response of the system and the vortex wake dynamics.

The only laminar flow, free-vibration experiment that we have encountered in the literature, was conducted by Anagnostopoulos and Bearman (1992). They indicate that the maximum amplitude occurred near the lower limit of the lock-in region.

Some researchers tried to simulate VIV of a circular cylinder numerically. Newman and Karniadakis (1997) performed a direct numerical simulation (DNS) study of the flow past a freely vibrating cable using body fitted coordinates at Reynolds numbers 100 and 200. Singh and Mittal (2005) simulated numerically VIV of a circular cylinder at low Reynolds numbers. They carried out two sets of computations to investigate the effect of Re and reduced natural frequency, F_n ($F_n=1/U^*$). They found that the effect of Re is very significant. Guilmineau and Quetery (2004) investigated VIV of a circular cylinder with low mass-damping in a turbulent flow using three sets of initial condition: (a) from rest, (b) increasing velocity and (c) decreasing velocity.

Some researchers studied the effect of mass and damping on the system response (Khalak and Williamson, 1997). Some of them suggest that the system response is characterized by combined mass-damping, $m^*\zeta$ (Griffin, 1980; Neudascher & Rockwell, 1993); on the other hand some researchers state that the system response is influenced by the independent effects of mass and

damping (Sarpkaya, 1995).

Much research on this subject is discussed in the review by Williamson and Govardhan (2004).

To date the majority of studies of VIV of a cylinder have been experimental and at Reynolds numbers where the flow is inherently turbulent and three dimensional. The only laminar flow, free vibration experiment that we have encountered in the literature is by Anagnostopoulos and Bearman (1992). In this study we numerically simulated their experiment and investigated the behavior of dynamic response of the system. More specifically, we investigate the effect of mass ratio and damping ratio on the system response.

2. NUMERICAL APPROACH

To find the system response, we should solve the Navier-Stokes equations, calculate the fluid force applied to the cylinder, and then solve the cylinder equation of motion.

The governing equations for the incompressible flow of a Newtonian fluid are the Navier-Stokes and continuity equations, which for two-dimensional flows can be expressed in terms of vorticity and stream-function as follows:

$$\frac{\partial \omega}{\partial t} + \left(\vec{u}.\vec{\nabla}\right)\omega = \nu \nabla^2 \omega \qquad (1)$$

$$\nabla^2 \psi = -\omega \qquad (2)$$

where ω, ψ and $\vec{u}$ are the vorticity, stream-function and velocity vector, respectively, and ν is the kinematic viscosity of the fluid. Equation (2) is the Poisson equation for stream function which replaces the continuity equation. We use a vortex method to solve the vorticity equation, Equation (1). An "operator splitting" method is applied to solve this equation. In this method the vorticity transport equation is splitted into the convection and diffusion parts as follows:

$$\frac{\partial \omega}{\partial t} = -(\vec{u}.\vec{\nabla})\omega \qquad (3)$$

$$\frac{\partial \omega}{\partial t} = \nu \nabla^2 \omega \qquad (4)$$

The vorticity field is discretized into a number of point vortices, and the time domain is also discretized into small time steps. Equation (3) states that the total derivative of vorticity is zero during "convection", or that the vorticity of a particle is constant as convected with the local velocity. Hence, in the "convection" part, the vortex particles are convected with the local velocity for a short period of a time step. To determine the velocity field, Equation (2) is solved for the stream function (given the vorticity field), and the velocity field is then computed as the curl of stream function. Next, the diffusion process is simulated by solving Equation (4) using a second order ADI finite difference scheme. The "no-flow" boundary condition is satisfied during the solution of convection problem, and the "no-slip" boundary condition is satisfied by the creation of new vorticiy on the body surface during each time-step. The force acting on the cylinder is due to both the pressure and shear stress distributions. In order to calculate the surface pressure, the Navier-Stokes equation in the radial direction is used, as discussed by Akbari (1999). Having obtained the velocity field, the skin friction on the cylinder surface is also obtained from a finite difference approximation. The drag and lift are obtained by integrating the pressure and skin friction around the cylinder surface. For more details on the numerical method applied in this investigation, refer to Akbari (1999) and Akbari and Price (2005).

The transverse response of the cylinder, $y(t)$, to the fluid force, $F_y(t)$, is modeled using a mass, spring and damper model. The cylinder's equation of transverse motion is given by:

$$m\ddot{y} + c\dot{y} + ky = F_y \qquad (5)$$

where, m is the cylinder mass, c the damping coefficient, k the structural stiffness, y the transverse cylinder displacement, and F_y is the transverse fluid force on the cylinder. Having calculated the transverse force, we use a fourth-order Runge-Kutta scheme to solve Equation (5), for the cylinder displacement.

3. RESULTS

In VIV of a cylinder the fluctuating force originating from vortex shedding causes the cylinder to vibrate. Therefore, before simulating VIV, we should make certain that the magnitude and frequency of the periodic forces on the cylinder are calculated with acceptable accuracy.

For this purpose, we investigated the flow past a fixed cylinder at different Reynolds numbers (80<Re<200). In each case we obtained the mean drag coefficient, $\overline{C}_D$, the amplitude of lift coefficient, C'_L, and the Strouhal number, St, (St=$f_v U/D$). A power spectrum analysis is applied to find the frequency of vortex shedding. To check the accuracy of our results, we compare the results with previous available data. The results for Re=100 are

compared in Table 1 with available data, where an acceptable agreement is observed.

Table 1: *Comparison of results for a fixed cylinder at Re = 100.*

	C_L'	$\overline{C}_D$	St
Anagnostopoulos (1994)	0.27	1.20	0.167
Henderson (1995)	0.33	1.35	0.166
Shiels et al. (2001)	0.33	1.33	0.167
Present results	0.33	1.33	0.163

To check the accuracy of our results for other Re numbers, we investigated the variation of St with Re and compared these results with the "universal" Strouhal-Reynolds number relation given by Williamson (1988). These are as presented in Figure 1, where a good agreement is observed.

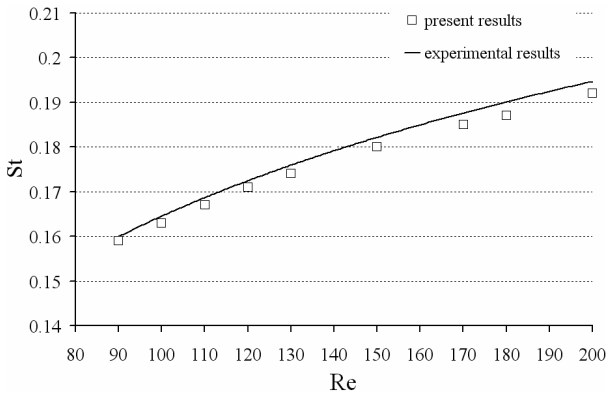

Figure 1: *Variation of St versus Reynolds number for a fixed cylinder; experimental results from Williamson (1988).*

In this work vortex induced vibration of an elastically supported circular cylinder at low Reynolds numbers is numerically investigated. As mentioned before, to date the majority of studies of VIV of the cylinder have been at a Reynolds number where the flow is inherently turbulent and three dimensional. The only laminar flow, free vibration experiment that we have seen in the literature is by Anagnostopoulos and Bearman (1992). We decided to simulate their experiment numerically, and then investigate the changes in system responses with variation of mass ratio and damping ratio.

Therefore, first we set the system parameters corresponding to what Anagnostopoulos and Bearman (1992) used in their experiments: m^*=149, f_n=7.016, ζ=0.0012. The reduced velocity range is 5 to 9. The changes to reduced velocity is achieved by altering the flow speed, and thus the Reynolds number will also change according to Re=17.9U^*; therefore, the Reynolds number changes from 90 to 160 in these simulations.

At the start of each simulation the cylinder was held fixed at its equilibrium position until a periodic flow was established. For each reduced velocity we investigated the time history of cylinder displacement and the lift force on the cylinder. Applying a power spectrum analysis, vortex shedding and cylinder oscillation frequencies are obtained and are checked for lock-in phenomenon.

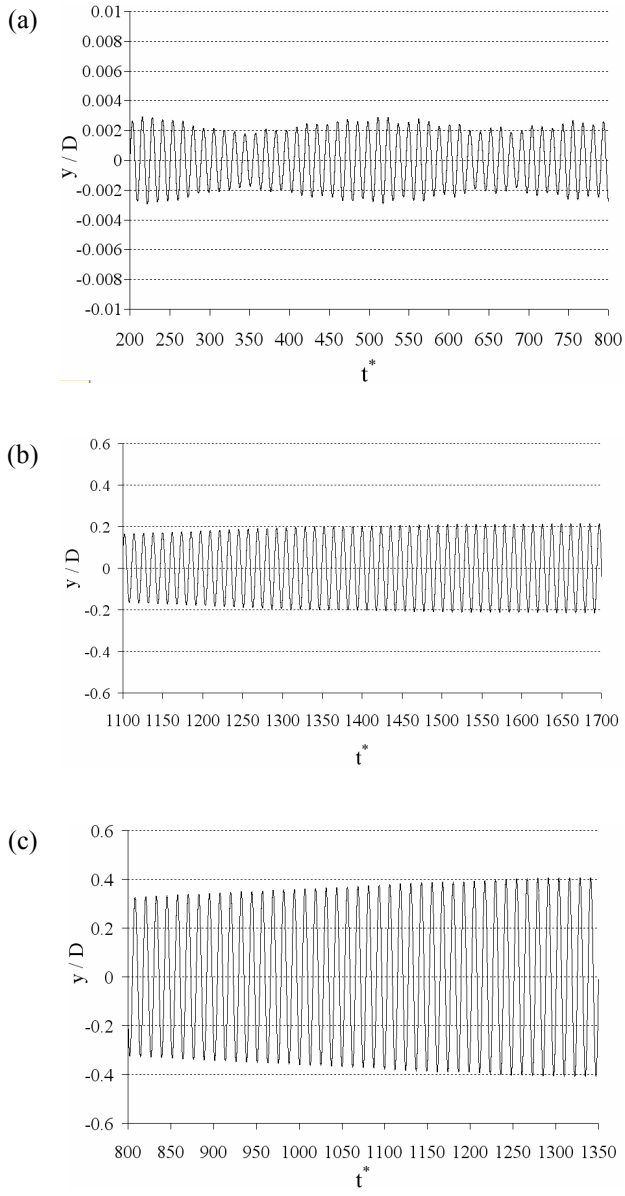

Figure 2: *Displacement response of the cylinder at: (a) Re = 90, (b) Re = 105, (c) Re = 110.*

Figure 2 presents the displacement histogram of the cylinder displacement for three different U^* (and hence Re). Part (a) of the figure corresponds to U^*=5.03 (Re=90). As seen in the figure, the vibration amplitude of the cylinder is very small in this case. Lock-in does not occur in this case, since

a PDS analysis of the lift force indicates that the vortex shedding occurs at its natural frequency for a stationary cylinder. Moreover, we can see that a beating effect is present in the results of our two-dimensional analysis, which is in agreement with the experimental results by Anagnostopoulos and Bearman (1992).

Increasing the reduced velocity (and hence Re), we will face a sudden change in the system response. The oscillation amplitude increases gradually before it reaches a steady value after many oscillation cycles. Another noticeable change is that in this case the vortex shedding frequency diverges from that for a stationary cylinder and becomes equal to the frequency of the cylinder oscillation. Figure 2(b) indicates one such case for U^*=5.87 (Re=105). Figure 4(c) shows similar results for a case with U^*=6.15 (Re=110). In this case also lock-in has occurred and the cylinder experiences high amplitude oscillation, but the amplitude is more than the previous case.

In Figure 3 the variation of the maximum amplitude with U^* and Re are presented and compared with the experimental results of Anagnostopoulos and Bearman (1992) as well as the numerical results of Anagnostopoulos (1994). Although there are some differences with the previous results, the general trend of the lock-in region is captured well. Unlike what is reported by Anagnostopoulos and Bearman (1992), we found the highest amplitude of oscillation near the middle of lock-in region. This is, however, in agreement with the results of Feng (1968).

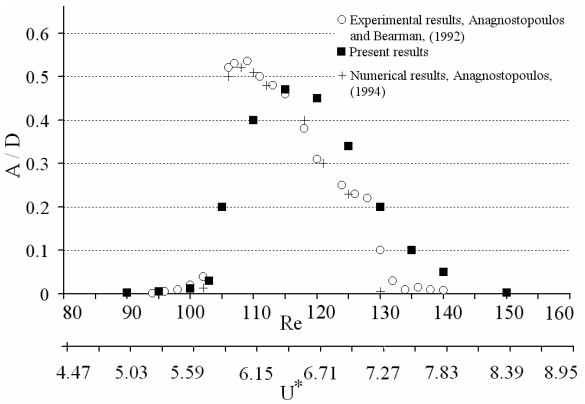

Figure 3: *Variation of maximum non-dimensional cylinder oscillation amplitude with Re.*

Nevertheless, the reduced velocity at which lock-in starts to occur and the reduced velocity band over which lock-in occurs is in good agreement with the experimental data.

Vortex induced vibration of a circular cylinder is in general a nonlinear phenomenon and the system response depends on a number of parameters including the reduced velocity, U^*, Reynolds number, Re, mass ratio, m^* and damping ratio, ζ. We intend to study the variation of system behavior due to changes in mass ratio and damping ratio.

To see the effect of mass ratio on the system response, we investigated three cases with m^*=298, 149, 74.5. In all these cases the damping ratio is held constant at ζ=0.0012. Figure 4 presents the variation of maximum cylinder oscillation amplitude with reduced velocity for these three cases with different mass ratios. It is observed that decreasing mass ratio results in an increase in the oscillation amplitude, and an increase in the reduced velocity over which lock in occurs.

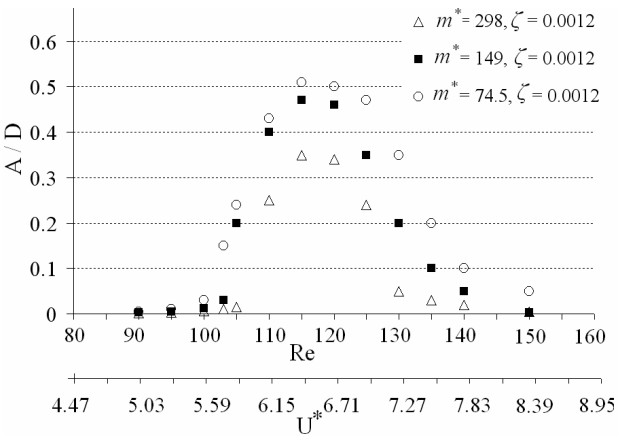

Figure 4: *Variation of maximum non-dimensional cylinder oscillation amplitude with Re for three cases with different mass-ratios.*

Referring to Figure 4 and considering the results of the case with m^*=74.5, we observe that the maximum attainable amplitude for this case is about 0.52 *D*. We observe that by doubling the mass-ratio to m^*= 149, the amplitude response of the system has slightly decreased, and the maximum amplitude decreased to 0.48 *D*. This should be compared with a case where the value of mass ratio is doubled again (increased from 149 to 298). It is seen that in this case there is a considerable change in the cylinder oscillation amplitude response, such that the maximum oscillation amplitude has decreased to 0.36 *D*. This shows that the changes in the system response due to mass-ratio variation are not linear in general.

We also investigated the effect of damping ratio on the system response. We considered three damping ratio, ζ = 0.0024, 0.0012, 0.0006. In all these cases m^*=149. Figure 5 presents the variation of maximum oscillation amplitude for three different damping ratios. We see that increasing

damping ratio decreases oscillation amplitude and the velocity rang over which lock-in occurs. Here again we see that the changes in the system response due to damping ratio variation are not linear.

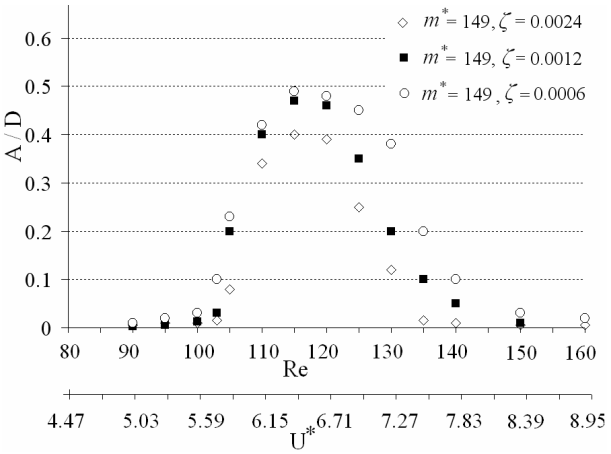

Figure 5: *Variation of maximum non-dimensional cylinder oscillation amplitude with Re for three cases with different damping-ratios.*

Comparing the results presented in Figures 4 and 5 for this range of Re number, mass ratio and damping ratio, it appears that the system response is not characterized by combined mass-damping parameter ($m^*\zeta$), unlike what was proposed by Griffin (1980). In other words, it can be observed that the mass ratio and damping ratio have independent influences on the system response. It is also found that the system is more dependent on mass ratio.

Considering the case with m^*=149 and ζ=0.0012 as the base case, we can double $m^*\zeta$ by either doubling m^* (to 298) or doubling ζ (to 0.0024). Comparing the results of these two cases (the case with m^*=298, ζ=0.0012 and the case with m^*=298, ζ=0.0012) with the base case (with m^*=149, ζ=0.0012), it is observed that the mass ratio exhibits more influence on the oscillation amplitude such that the changes are more considerable.

The vorticity field for each case was also investigated. Figure 6 shows the instantaneous vorticty field at four selected Reynolds numbers for the case with m^*=149 and ζ=0.0012. For all the range of Reynolds numbers considered here, vortex shedding is of 2S type (two oppositely vortices are shed per cycle). Parts (a) and (d) of the figure show the vorticity contours for Re=100 and Re=150 respectively, where lock-in did not occur. The vorticity contours in these cases are very similar to those for a fixed cylinder at the same Reynolds numbers. Parts (b) and (c) of the figure show vorticity contours for two cases where lock-in has occurred. Comparing with the contours for a fixed cylinder at the same Re, we see that vortex spacing is smaller for the oscillating cylinder. It shows that that the vortex shedding frequency diverges from that predicted by the Strouhal relation. In these cases the vortices in the wake coalesce giving rise to the C(2S) mode of vortex shedding (as described by Williamson and Roshko, 1988). The C(2S) is very similar to the 2S mode except that vortices coalesce in far wake.

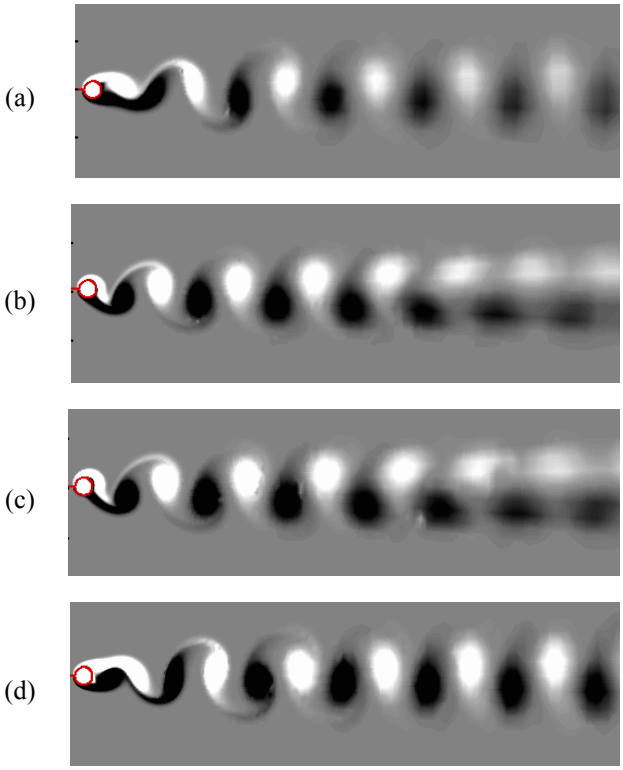

Figure 6: *Instantaneous vorticity contours for a free-vibrating circular cylinder at different Reynolds numbers for the case with m^*=149 and ζ=0.0012: (a) Re=90; (b) Re=105; (c) Re=110; (d) Re=150.*

4. CONCLUSION

The flow induced vibration of a low-damped elastically mounted circular cylinder in laminar flow was simulated using a two dimensional vortex method. Our main purpose in this work was to investigate the system response due to changes in mass ratio and damping ratio in low-Reynolds number regime. We simulated a case for which experimental results are available and found acceptable agreement. We also investigated the system response due to changes in mass ratio and damping ratio. It is found that in the present range

of Reynolds number, mass ratio and damping ratio, the system response is governed by mass ratio and damping ratio independently. In the synchronization regime at low Reynolds numbers we found the 2S or C(2S) type vortex shedding, unlike the 2P or S+P types which are observed in the turbulent flow regime.

5. REFERENCES

Akbari, M.H., 1999, Bluff-Body Flow Simulations Using Vortex Methods. Ph.D. thesis, Department of Mechanical Engineering, McGill University, Montréal, Canada.

Akbari, M.H., Price, S.J., 2005, Numerical investigation of flow patterns for staggered cylinder pairs in cross-flow. *Journal of Fluids and Structures,* **20**: *533-554*.

Anagnostopoulos, P., 1994, Numerical investigation of response and wake characteristics of a vortex excited cylinder in a uniform stream. *Journal of Fluids and Structures*, **8**: 367-390, 1994.

Anagnostopoulos, P., Bearman, P.W., 1992, Response characteristics of a vortex-excited cylinder at low Reynolds numbers. *Journal of Fluids and Structures*, **6**: 39-50.

Brika, D., Laneville, A., 1993, Vortex-induced vibration of a long flexible circular cylinder. *Journal of Fluid Mechanics*, **250**: 481-508.

Feng, C.C., 1968, The measurement of vortex-induced effects in flow past stationary and oscillating circular and d-section cylinders. M.A.Sc. thesis, University of British Columbia, Vancouver, B.C., Canada.

Gharib, M.R., 1999, Vortex-induced vibration, absence of lock-in and fluid force deduction. Ph.D. thesis, California Institute of Technology, CA, USA.

Griffin, O.M., 1980, Vortex-excited cross flow vibrations of a single cylindrical tube. *Journal of Pressure Vessel Technology,* **102**: 158-166.

Guilmineau, E., Queutey, P., 2004, Numerical simulation of vortex-induced vibration of a circular cylinder with low mass-damping in a turbulent flow. *Journal of Fluid and Structures*, **19**: 449-466.

Henderson, R.D., 1995, Details of the drag curve near the onset of vortex shedding. *Physics of Fluids*, **7**: 2102-2104.

Jauvtis, N., Williamson, C.H.K. 2003, Vortex-induced vibration of cylinder with two degree of freedom. *Journal of Fluids and Structures*, **17**: 1035-1042.

Khalak, A, Williamson, C.K.H, 1997, Investigation of relative effects of mass and damping in vortex-induced vibration of a circular cylinder. *Journal of Wind Engineering and Industrial Aerodynamics* **69-71:** 341-350.

Khalak, A, Williamson, C.K.H, 1999, Motion, forces and mode transitions in vortex-induced at low mass-damping. *Journal of Fluids and Structures,* **13**: 813-851.

Naudascher, E., Rockwell, D., 1993 Flow-Induced Vibartion: An Engineering Guide. Rotterdam. .

Newman, D.J., Karniadakis, G.E., 1997, A direct numerical simulation study of flow past a freely vibrating cable. *Journal of Fluid Mechanics,* **136**: 344-395.

Sarpkaya, T., 1995, Hydrodynamic damping, flow-induced oscillation and biharmonic response. *ASME Journal of Offshore Mechanics and Arctic Engineering*, **117**: 232-238.

Shiels, D., et al, 2001, Flow-induced vibration of circular cylinder at limiting structural parameters *Journal of Fluids and Structures*, **15**: 3-21.

Singh, S.P., Mittal, S., 2005, Vortex-induced oscillations at low Reynolds numbers: Hysteresis and vortex-shedding modes. *Journal of Fluids and Structures*, **20**: 1085-1104.

Williamson, C.H.K., 1988. Defining a universal and continuous Strouhal-Reynolds number relationship for the laminar vortex shedding of a circular cylinder. *Physics of Fluids*, **31**: 2742-2744.

Williamson, C.H.K., Govardhan, R., 2004, Vortex-induced vibrations. *Annual Review of Fluid Mechanics,* **36**: 413-455.

Williamson, C.H.K., Roshko, A. 1988, Vortex formation in the wake of an oscillating cylinder. *Journal of Fluids and Structures,* **2**: 355–381.